two consecutive Fibonacci numbers as an approximant for the *irrational* τ in the quasicrystals (Zhang & Kuo, 1990; Kuo, 1993). Therefore, these crystalline phases are called approximants of a decagonal quasicrystal. Pentagons also exist in hexagonal crystals, such as the μ-Al_4Mn phase (Shoemaker, 1993), and this had been discussed together with the structural model of the Al–Mn decagonal quasicrystal.

The authors wish to thank the Chinese Academy of Sciences and the National Natural Science Foundation of China for financial support. XZL is also grateful to the Postdoctoral program of China for a grant.

References

BARBIER, J.-N., TAMURA, N. & VERGER-GAUGRY, J. L. (1993). *J. Non-Cryst. Solids*, **153, 154**, 126–131.

BLACK, P. J. (1955*a*). *Acta Cryst.* **8**, 43–48.

BLACK, P. J. (1955*b*). *Acta Cryst.* **8**, 175–182.

DONG, C., DUBOIS, J. M., KANG, S. S. & AUDIER, M. (1992). *Philos. Mag. B*, **65**, 107–126.

GRIN, J., BURKHARDT, U. & ELLNER, M. (1994). *J. Alloys Comp.* **206**, 243–247.

GRÜNBAUM, B. & SHEPHARD, G. C. (1987). *Tiling and Patterns*. San Francisco: Freeman.

HENLEY, C. L. (1985). *J. Non-Cryst. Solids*, **75**, 91–96.

HIRAGA, K., KANEKO, M., MATSUO, Y. & HASHIMOTO, S. (1993). *Philos. Mag. B*, **67**, 193–205.

HIRAGA, K., SUN, W. & LINCOLN, F. J. (1991). *Jpn. J. Appl. Phys.* **30**, L302–L305.

HUDD, R. C. & TAYLOR, W. H. (1962). *Acta Cryst.* **15**, 441–442.

KANG, S. S., MALAMAN, B., VENTURINI, G. & DUBOIS, J. M. (1992). *Acta Cryst.* **B48**, 770–776.

KUMAR, V., SAHOO, D. & ATHITHAN, G. (1986). *Phys. Rev. B*, **34**, 6924–6932.

KUO, K. H. (1993). *J. Non-Cryst. Solids*, **153/154**, 40–44.

LI, X. Z., MA, X. L. & KUO, K. H. (1994). *Philos. Mag. Lett.* **70**, 221–229.

LI, X. Z., SHI, D. & KUO, K. H. (1992). *Philos. Mag. B*, **66**, 331–340.

LI, H. L., ZHANG, Z. & KUO, K. H. (1994). *Phys. Rev. B*. In the press.

MA, X. L. & KUO, K. H. (1992). *Metall. Trans A*, **23**, 1121–1128.

MA, X. L. & KUO, K. H. (1994). *Metall. Mater. Trans. A*, **25**, 47–56.

MA, X. L. & KUO, K. H. (1995). *Metall. Mater. Trans A*. In the press.

PENROSE, R. (1974). *Bull. Inst. Math. Appl.* **10**, 266–271.

SHI, N. C., LI, X. Z., MA, Z. S. & KUO, K. H. (1994). *Acta Cryst.* **B50**, 22–30.

SHOEMAKER, C. B. (1993). *Philos. Mag. B*, **67**, 869–881.

STEURER, W. & KUO, K. H. (1990). *Acta Cryst. B*, **46**, 703–712.

TSUCHIMORI, M., ISHIMASA, T. & FUKANO, Y. (1992). *Philos. Mag. B*, **66**, 89–108.

ZHANG, H. & KUO, K. H. (1990). *Phys. Rev. B*, **42**, 8907–8914.

Acta Cryst. (1995). B**51**, 43–47

Single-Crystal Pulsed Neutron Diffraction Structure of the Antiferromagnet $K_2[FeCl_5(H_2O)]$ With and Without Applied Pressure*

BY ARTHUR J. SCHULTZ

Intense Pulsed Neutron Source, Argonne National Laboratory, Argonne, IL 60439, USA

AND RICHARD L. CARLIN

Department of Chemistry, The University of Illinois at Chicago, Chicago, IL 60607, USA

(*Received* 15 *February* 1994; *accepted* 18 *July* 1994)

Abstract

The crystal structure of $K_2[FeCl_5(H_2O)]$ was examined at 15 K and ambient pressure (1 bar = 0.1 MPa) and at 15 K and 0.14 GPa (1.4 kbar) by single-crystal time-of-flight neutron diffraction in order to search for structural changes coincident with the discontinuity in the slope of the spin-flop transition field (H_{SF}) *versus* pressure at 60 MPa. It is found that intramolecular and hydrogen-bond distances and angles are statistically equivalent at the two pressures. However, there are significant changes of as much as 0.049 (3) Å in the intramolecular Cl···Cl distances which may affect the Fe—Cl···Cl—Fe superexchange pathways and the discontinuity in H_{SF}. Dipotassium aquapentachloroferrate(III), M_r = 329.3, $F(000)$ = 636, orthorhombic, *Pnma*, Z = 4. At 15 K and ambient pressure (0.1 MPa), a = 13.452 (5), b = 9.631 (2), c = 7.003 (2) Å, V = 907.3 (5) Å^3, D_x = 2.41 g cm^{-3}. At 15 K and 0.14 GPa, a = 13.391 (4), b = 9.648 (2), c = 6.942 (2) Å, V = 896.9 (4) Å^3, D_x = 2.44 g cm^{-3}. The a and c axes decrease slightly, whereas the b axis increases slightly, under applied pressure.

* The author of this manuscript is a contractor of the US Government under contract No. W-31-109-ENG-38. Accordingly, the US Government retains a non-exclusive, royalty-free license to publish or reproduce the published form of this contribution, or allow others to do so, for US Government purposes.

Introduction

The series of compounds $A_2[FeX_5(H_2O)]$ (A = K, Rb, Cs, and NH_4; X = Cl and Br) have been extensively

studied because of their interesting magnetic properties (Carlin & Palacio, 1985). The salts order antiferromagnetically with transition temperatures T_c ranging from *ca* 6 to 23 K. These ordering temperatures are unusually high for discrete, hydrated, metal complexes involving superexchange pathways of the type Fe—$X\cdots X$—Fe and Fe—O—H$\cdots X$—Fe. That is, the metal ions are not directly connected by covalently bonded atoms, such as an Fe—O—Fe or Fe—Cl—Fe linkage. The iron(III) ions in these compounds are in high spin, $S = 5/2$ states, exhibit weak magnetic anisotropy, and therefore are good examples of the Heisenberg model. Except for $Cs_2[FeX_5(H_2O)]$, the compounds are all isomorphous.

The $K_2[FeCl_5(H_2O)]$ salt has a zero applied-field critical temperature $T_c(0)$ of 14.06 K (McElearney & Merchant, 1978). An investigation of the boundaries between the paramagnetic, antiferromagnetic, and spin-flop phases in the H–T phase diagram shows the bicritical point at 13.6 K and 34.1 kOe (Palacio, Paduan-Filho & Carlin, 1980). From single-crystal Mössbauer measurements in an applied magnetic field it is deduced that the spins are aligned along the a axis in the antiferromagnetic phase and along the c axis in the spin-flop phase (Karki & Hall, 1993). $K_2[FeCl_5(H_2O)]$ is also of particular interest due to the unusual pressure dependence of its spin-flop transition field, H_{SF}, as reported by Ortiz, Paduan-Filho & Missell (1980, 1981). H_{SF} decreases sharply ($dH_{SF}/dP \simeq -18$ kOe GPa^{-1}) up to 60 MPa. At 60 MPa there appears to be a sharp discontinuity in the slope of H_{SF} *versus* pressure ($dH_{SF}/dP \simeq -20$ kOe GPa^{-1}), indicative of some type of phase transition. In addition, comparison with the isomorphous Rb salt suggests that H_{SF} should *increase* with applied pressure due to the assumed contraction of the lattice. Thus, it has been proposed (Ortiz, Paduan-Filho & Missell, 1981) that the decrease in H_{SF} with pressure could be due to a subtle change in the coordination geometry of the iron. In this paper we describe the single-crystal neutron diffraction structure of $K_2[FeCl_5(H_2O)]$ at low temperature with and without applied pressure in order to identify any changes.

Experimental

Neutron data collection

Large single crystals ($\sim$3 mm^3) were obtained by slow evaporation from a 1:2 molar ratio solution of $FeCl_3.6H_2O$ and KCl in dilute hydrochloric acid. Time-of-flight neutron diffraction data were obtained at the Intense Pulsed Neutron Source (IPNS) at Argonne National Laboratory using the single-crystal diffractometer equipped with a position-sensitive ^{6}Li-glass scintillation area (30 × 30 cm) detector (Schultz, 1987). At the IPNS, pulses of protons are accelerated into a heavy-element target 30 times a second to produce pulses of neutrons by the spallation process. Because of the pulsed nature of the source, neutron wavelengths are determined by time-of-flight based on the de Broglie equation $\lambda = (h/m)(t/l)$, where h is Planck's constant, m is the neutron mass, and t is the time-of-flight for a flight path l, so that the entire thermal spectrum of neutrons can be used. With an area position-sensitive detector and a range of neutron wavelengths, a solid volume of reciprocal space is sampled with a stationary orientation of the sample and the detector. Details of the data collection and analysis procedures have been provided previously (Schultz, Van Derveer, Parker & Baldwin, 1990). Table 1 contains a summary of the data collection, analysis and refinement parameters for this experiment.

Table 1. *Unit-cell, data collection and refinement parameters for* $K_2[FeCl_5(H_2O)]$

	15 K, 0.1 Mpa	15 K, 0.14 GPa
a (Å)	13.452 (5)	13.391 (4)
b (Å)	9.631 (2)	9.648 (2)
c (Å)	7.003 (2)	6.942 (2)
V (Å^3)	907.3 (5)	896.9 (4)
Space group	Orthorhombic *Pnma*	
Z	4	
Radiation	Neutrons	
Wavelength range (Å)	0.7–4.2 determined by time-of-flight	
Data-collection technique	Time-of-flight Laue with 30 × 30 cm position-sensitive area detector	
Linear absorption coefficient $\mu(\lambda)$ (cm^{-1})	$0.64 + 0.60\lambda$	
Absorption correction (cm)	Spherical, $r = 0.09$	
Function minimized	$\sum w(\lvert F_o\rvert - \lvert F_c\rvert)^2$	
No. of reflections ($F^2 > 3\sigma$)	2018	1891
$R(F)$	0.057	0.054
$wR(F)$	0.052	0.050
GOF	1.08	1.06

Temperature and pressure were controlled using a helium gas pressure cell mounted on the cold stage of a Displex® closed-cycle helium refrigerator (Air Products and Chemicals, Inc., Model CS-202). The crystal in the pressure cell was immersed in the fluorinated hydrocarbon Fluorinert® (3M Company) in order to provide hydrostatic pressure conditions. For the first data collection, the cell was pressurized to 0.14 GPa and cooled to 15 ±1 K. It was then warmed to room temperature, the pressure was released, and the crystal was cooled to 15 ±1 K for the second data set.

An orientation matrix was initially obtained by an auto-indexing procedure using data obtained by searching a histogram for peaks (Jacobson, 1986). 15 diffractometer settings were used for both the high- and low-pressure data collections to obtain at least one unique quadrant of reciprocal space. For each setting of the diffractometer angles, data were stored in three-dimensional histogram form with coordinates x, y, t corresponding to horizontal and vertical detector positions and the time-of-flight, respectively. The 120 time-of-flight histogram channels were constructed with constant $\Delta t/t = 0.015$ and correspond to wavelengths of 0.7–4.2 Å. Bragg reflections were integrated about their

Table 2. *Atomic coordinates and anisotropic thermal parameters for* $K_2[FeCl_5(H_2O)]$

First line: $T = 15$ K, $P = 0.1$ MPa (ambient pressure). Second line: $T = 15$ K, $P = 0.14$ GPa.

The expression for the anisotropic temperature factor is $\exp[-2\pi^2(a^{*2}U_{11}h^2 + b^{*2}U_{22}k^2 + c^{*2}U_{33}l^2 + 2a^*b^*U_{12}hk + 2a^*c^*U_{13}hl + 2b^*c^*U_{23}kl)]$.

	x	y	z
K	0.3538 (2)	0.0023 (3)	0.8540 (3)
	0.3544 (2)	0.0025 (2)	0.8517 (3)
Fe	0.1141 (1)	1/4	0.8061 (2)
	0.1150 (1)	1/4	0.8057 (2)
Cl(1)	0.2186 (1)	1/4	1.0785 (2)
	0.2202 (1)	1/4	1.0785 (2)
Cl(2)	0.2525 (1)	1/4	0.6043 (2)
	0.2527 (1)	1/4	0.6021 (2)
Cl(3)	0.0062 (1)	1/4	0.5326 (2)
	0.0057 (1)	1/4	0.5320 (2)
Cl(4)	0.10447 (8)	0.00376 (7)	0.8141 (1)
	0.10489 (7)	0.00392 (7)	0.8145 (1)
O	−0.0088 (2)	1/4	0.9839 (3)
	−0.0081 (2)	1/4	0.9857 (3)
H	−0.0350 (4)	0.3314 (3)	1.0441 (5)
	−0.0356 (3)	0.3311 (3)	1.0452 (6)

	U_{11}	U_{22}	U_{33}	U_{12}	U_{13}	U_{23}
K	0.0089 (10)	0.0079 (6)	0.0097 (7)	0.0004 (8)	−0.0014 (8)	0.0003 (6)
	0.0071 (9)	0.0083 (6)	0.0087 (7)	−0.0005 (7)	−0.0010 (7)	0.0015 (6)
Fe	0.0062 (6)	0.0043 (3)	0.0061 (4)	0	0.0010 (5)	0
	0.0042 (5)	0.0047 (3)	0.0060 (4)	0	0.0003 (4)	0
Cl(1)	0.0070 (6)	0.0087 (4)	0.0067 (4)	0	−0.0014 (4)	0
	0.0064 (5)	0.0091 (4)	0.0059 (5)	0	−0.0016 (4)	0
Cl(2)	0.0053 (5)	0.0069 (4)	0.0068 (4)	0	0.0010 (5)	0
	0.0043 (5)	0.0083 (4)	0.0058 (4)	0	0.0012 (5)	0
Cl(3)	0.0068 (6)	0.0077 (4)	0.0082 (5)	0	−0.0014 (5)	0
	0.0073 (6)	0.0076 (4)	0.0065 (5)	0	−0.0006 (5)	0
Cl(4)	0.0077 (4)	0.0053 (2)	0.0095 (3)	0.0001 (3)	0.0020 (4)	0.0004 (3)
	0.0080 (4)	0.0056 (2)	0.0081 (3)	0.0000 (3)	0.0021 (3)	0.0003 (3)
O	0.0102 (11)	0.0071 (5)	0.0132 (8)	0	0.0067 (9)	0
	0.0097 (10)	0.0076 (5)	0.0108 (8)	0	0.0048 (8)	0
H	0.035 (2)	0.017 (1)	0.033 (2)	0.003 (1)	0.007 (2)	−0.0076 (9)
	0.031 (2)	0.019 (1)	0.035 (2)	0.006 (1)	0.009 (2)	−0.008 (1)

predicted location and were corrected for the Lorentz factor, the incident spectrum, the detector efficiency and dead-time losses. A wavelength-dependent spherical absorption correction was applied (Howard, Johnson, Schultz & Stringer, 1987). Symmetry-related reflections were not averaged since different extinction factors were applicable to reflections measured at different wavelengths.

Solutions and refinements of the structures

The initial non-H-atom positional coordinates for the structure were obtained from the room-temperature X-ray structure of the isomorphous $Rb_2[FeCl_5(H_2O)]$ (O'Connor, Deaver & Sinn, 1979). The H-atom position was obtained from a difference Fourier map. Atomic scattering lengths used in the least-squares refinements were those tabulated by Sears (Sears, 1986). The observations were weighted according to $w = (\sigma_{cs}^2 + P^2|F|^4 + Q)^{-1}$ with σ_{cs}^2 = counting statistical variance, $P = 0.04$ (instrumental imprecision), Q = constant. Q accounts for systematic errors which are common to all data points, *e.g.* common background errors. In practice, its effect is small in comparison to the random uncertainties, as it only reduces the weights of the weakest reflections, which also yields a value near unity for GOF = $[\sum w||F_o| - |F_c||^2/(N_o - N_v)]^{1/2}$, where N_o = number of observations, N_v = number of variables. In the final cycles of least-squares refinements, all atoms were treated with anisotropic temperature factors and a secondary extinction correction [Becker & Coppens (1974) formalism, type I, Lorentzian distribution] was included. Table 2 contains the final atomic coordinates and anisotropic temperature factors.*

Results and discussion

The single-crystal neutron structure of $K_2[FeCl_5(H_2O)]$ was determined at 15 K at ambient pressure (0.1 MPa) and at 15 K with an applied hydrostatic pressure of 0.14 GPa. The a and c axes contract slightly due to pressure, whereas the b axis is 0.017 (3) Å longer at the higher pressure. This results in a 1% contraction of the unit-cell volume. Interatomic distances and angles and the differences between the 0.1 MPa and 0.14 GPa structures are given in Table 3.

* Lists of structure factors have been deposited with the IUCr (Reference: CR0474). Copies may be obtained through The Managing Editor, International Union of Crystallography, 5 Abbey Square, Chester CH1 2HU, England.

Table 3. *Interatomic distances* (Å), *angles* (°) *and differences* (0.1 MPa–0.14 GPa)

	15 K, 0.1 MPa	15 K, 0.14 GPa	Difference
Fe coordination geometry			
Fe—O	2.070 (3)	2.068 (3)	0.002 (4)
Fe—Cl(1)	2.369 (2)	2.361 (2)	0.008 (3)
Fe—Cl(2)	2.337 (2)	2.323 (2)	0.014 (3)
Fe—Cl(3)	2.403 (2)	2.398 (2)	0.005 (3)
Fe—Cl(4) (× 2)	2.3757 (9)	2.3788 (8)	−0.003 (1)
O—Fe—Cl(1)	89.40 (10)	89.48 (9)	−0.08 (14)
O—Fe—Cl(2)	179.7 (1)	179.7 (1)	0.0 (1)
O—Fe—Cl(3)	89.8 (1)	89.6 (1)	0.2 (1)
O—Fe—Cl(4) (× 2)	86.67 (4)	86.52 (4)	0.15 (6)
Cl(1)—Fe—Cl(2)	90.85 (8)	90.80 (7)	0.05 (10)
Cl(1)—Fe—Cl(3)	179.21 (9)	179.07 (8)	0.14 (12)
Cl(1)—Fe—Cl(4) (× 2)	90.77 (4)	90.75 (4)	0.02 (6)
Cl(2)—Fe—Cl(3)	89.94 (7)	90.13 (7)	−0.19 (10)
Cl(2)—Fe—Cl(4) (× 2)	93.32 (4)	93.48 (4)	−0.16 (6)
Cl(3)—Fe—Cl(4) (× 2)	89.19 (4)	89.19 (4)	0.00 (6)
Cl(4)—Fe—Cl(4)	173.16 (8)	172.86 (7)	0.30 (10)
H—atom distances and angles			
O—H	0.958 (3)	0.959 (3)	−0.001 (4)
H—O—H	110.0 (6)	109.4 (5)	0.6 (8)
Fe—O—H (× 2)	124.0 (3)	124.5 (3)	−0.5 (4)
H···Cl(4^{i})	2.148 (3)	2.142 (3)	0.006 (4)
O—H—Cl(4)	175.1 (5)	176.2 (4)	−1.1 (6)
O···Cl(4^{i})	3.103 (2)	3.099 (2)	0.004 (3)
Intramolecular Cl···Cl distances less than 4.7 Å (ascending order)			
Cl(1)···Cl(2^{ii})	3.710 (2)	3.661 (2)	0.049 (3)
Cl(2)···Cl(4$^{iii, iv}$) (× 2)	3.715 (2)	3.692 (1)	0.023 (2)
Cl(3)···Cl(4$^{v, vi}$) (× 2)	3.753 (1)	3.739 (1)	0.014 (1)
Cl(1)···Cl(4$^{vii, viii}$) (× 2)	3.789 (2)	3.764 (1)	0.025 (2)
Cl(4)···Cl(4^{ix})	3.832 (2)	3.812 (2)	0.020 (3)
Cl(1)···Cl(3^{x})	3.947 (3)	3.899 (2)	0.048 (4)
Cl(2)···Cl(3^{x})	4.256 (3)	4.235 (2)	0.021 (4)
Cl(1)···Cl(3^{xi})	4.275 (2)	4.262 (2)	0.013 (3)
K···Cl distances (ascending order)			
K···Cl(3^{xi})	3.244 (3)	3.234 (3)	0.010 (4)
K···Cl(1^{iii})	3.252 (3)	3.245 (3)	0.007 (4)
K···Cl(2)	3.257 (3)	3.249 (3)	0.008 (4)
K···Cl(4^{vii})	3.272 (2)	3.259 (2)	0.013 (3)
K···Cl(3^{vii})	3.319 (3)	3.319 (3)	0.000 (4)
K···Cl(2^{vii})	3.320 (3)	3.319 (3)	0.001 (4)
K···Cl(4)	3.366 (3)	3.351 (3)	0.015 (4)
K···Cl(1)	3.387 (3)	3.377 (3)	0.010 (4)

Symmetry codes: (i) $-x, \frac{1}{2}+y, 2-z$; (ii) $x, y, 1+z$; (iii) $\frac{1}{2}-x, -y, -\frac{1}{2}+z$; (iv) $\frac{1}{2}-x, \frac{1}{2}+y, -\frac{1}{2}+z$; (v) $-x, \frac{1}{2}+y, 1-z$; (vi) $-x, -y, 1-z$; (vii) $\frac{1}{2}-x, -y, \frac{1}{2}+z$; (viii) $\frac{1}{2}-x, \frac{1}{2}+y, \frac{1}{2}+z$; (ix) $-x, -y, 2-z$; (x) $\frac{1}{2}+x, \frac{1}{2}-y, \frac{1}{2}-z$; (xi) $\frac{1}{2}+x, \frac{1}{2}-y, -\frac{1}{2}-z$.

In the following discussion, distances and angles refer to the 15 K, 0.1 MPa structure followed by the 15 K, 0.14 GPa structure in brackets.

Fe *coordination geometry*

The coordination geometry about the Fe atom is distorted octahedral, as shown in Fig. 1. The Fe, O, Cl(1), Cl(2) and Cl(3) atoms sit on a crystallographic mirror plane at $y = 1/4$. Most *L*—Fe—*L'* angles are close to 90 or 180° except those involving Cl(4), which is bent away from Cl(2) and towards the water ligand {Cl(4)—Fe—O = 86.67 (4)° [86.52 (4)]}. This is also towards the direction of the hydrogen bond to a neighboring $[FeCl_5(H_2O)]^{2-}$ anion (*vide infra*). The Fe—O distances are 2.070 (3) Å [2.068 (3)]. Fe—Cl bond lengths range from 2.337 (2) [2.323 (2)] to 2.403 (2) Å [2.398 (2)]. The shortest Fe—Cl bond is to Cl(2), which is *trans* to the water ligand. The largest apparent change in bond lengths between the ambient pressure and the 0.14 GPa low-temperature structures is a small contraction of the Fe—Cl(2) bond [Δ = 0.014 (3) Å]. In addition, it is possible that Cl(4) bends slightly more away from Cl(2) and towards the O atom. However, all these changes are small and on the borderline of the experimental statistical significance, although changes of a few hundredths of an Ångstrom in the bond lengths may be sufficient to produce the observed magnetic properties.

Hydrogen bonding

The water ligand coordinates to the Fe atom, *trans* to Cl(2). The H_2O plane is slightly tilted out of the Fe–O–Cl(2)–Cl(4) plane towards Cl(1). Each H atom on the water ligand hydrogen bonds to a Cl(4) atom on a neighboring $[FeCl_5(H_2O)]^{2-}$ anion (Fig. 2), with

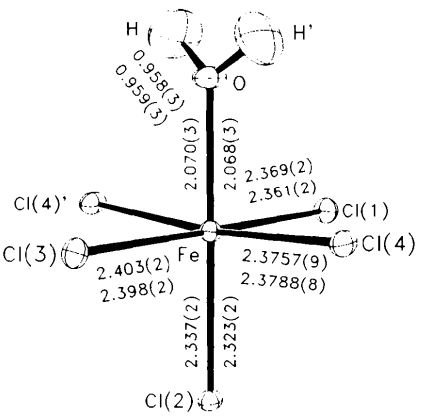

Fig. 1. Perspective drawing of the $[FeCl_5(H_2O)]^{2-}$ anion at 15 K and ambient pressure (0.1 MPa). Atoms are drawn at the 75% probability level. For each bond length (Å), the top number is for 15 K, 0.1 MPa and the lower number is for 15 K, 0.14 GPa.

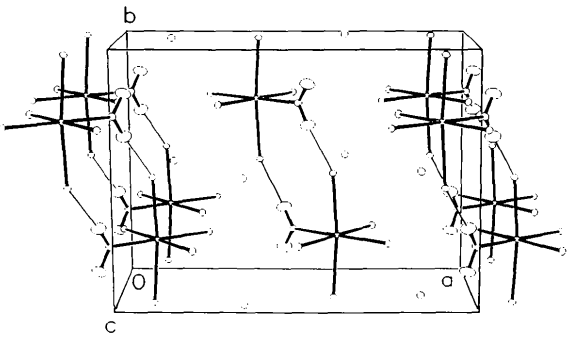

Fig. 2. Perspective view of the unit cell of $K_2[FeCl_5(H_2O)]$ at 15 K and ambient pressure (0.1 MPa). Atoms are drawn at the 50% probability level. H···Cl(4) hydrogen bonds are shown as thin lines.

H···Cl(4) = 2.148 (3) Å [2.142 (3)] and O—H···Cl(4) = 175.1 (5)° [176.2 (4)]. The hydrogen bond may account for the distortion of Cl(4) from its ideal octahedral site, since the distortion is towards the hydrogen bond and since Cl(1) and Cl(3) are also in the equatorial plane, but they are not hydrogen-bond acceptors and their angles are not distorted. The hydrogen bonds form one-dimensional chains of $[FeCl_5(H_2O)]^{2-}$ anions in the *b*-axis direction. Although the hydrogen bonds may play a role in the superexchange, there are virtually no statistically significant changes in the geometry of these bonds between the 0.1 MPa and the 0.14 GPa structures so that, within the precision of the experiment, there is no evidence that the hydrogen-bonding network is responsible for the change in the slope of H_{SF} *versus* pressure.

Intermolecular Cl···Cl *distances*

Intermolecular Cl···Cl distances in the range ~3.7–4.3 Å form a three-dimensional network of possible Fe—Cl···Cl—Fe superexchange pathways. The most statistically significant changes between the 0.1 MPa and 0.14 GPa structures are those involving Cl···Cl distances between neighboring $[FeCl_5(H_2O)]^{2-}$ anions. The largest changes occur for Cl(1)···Cl(2) and Cl(1)···Cl(3), with contractions of 0.049 (3) and 0.048 (4) Å, respectively, from ambient pressure to 0.14 GPa. Both of these interatomic vectors occur within the y = 0.25 plane, with the former being predominantly parallel to the c axis. Many of these changes listed in Table 3 are more than 10 e.s.d.'s and therefore one would predict an effect on superexchange *via* Fe—Cl···Cl—Fe pathways.

Concluding remarks

Although with only two data points it is not possible to observe a discontinuity, the absence of any pressure dependence in other parameters, coupled with the large changes in the Cl···Cl distances, indicates that the changes in the Cl···Cl distances (and the Fe—Cl···Cl—Fe superexchange pathways) may be partially responsible for the discontinuity in the slope of H_{SF} *versus* pressure. The reason for the negative value of the slope of H_{SF} *versus* pressure is still unclear since the isomorphous Rb analog $Rb_2[FeCl_5(H_2O)]$ has a unit cell which is larger and a $H_{SF}(0)$ which is smaller than that for the K salt. Thus, it would appear that the application of pressure should increase H_{SF} if there is a reduction in the unit-cell volume, which is the case. A reduction in the anisotropy of the Fe complex could explain these observations (Ortiz, Paduan-Filho & Missell, 1981). Within the experimental precision, our structural data does not appear to support evidence for a reduction in the distortion of the Fe coordination octahedron. However, under pressure the unit cell does not contract isotropically, such that the a and c axes contract slightly whereas the b axis expands slightly. Thus, there may be a subtle change in the anisotropy of the overall lattice which is difficult to evaluate.

Work at Argonne National Laboratory is supported by the Office of Basic Energy Sciences, Division of Materials Sciences, US Department of Energy, under Contract W-31-109-ENG-38.

References

BECKER, P. J. & COPPENS, P. (1974). *Acta Cryst.* **A30**, 129–147.
CARLIN, R. L. & PALACIO, F. (1985). *Coord. Chem. Rev.* **65**, 141–165.
HOWARD, J. A. K., JOHNSON, O., SCHULTZ, A. J. & STRINGER, A. M. (1987). *J. Appl. Cryst* **20**, 120–122.
JACOBSON, R. A. (1986). *J. Appl. Cryst.* **19**, 283–286.
KARKI, H. D. & HALL, I. (1993). *J. Phys. Condens. Matter*, **5**, 7751–7760.
MCELEARNEY, J. N. & MERCHANT, S. (1978). *Inorg. Chem.* **17**, 1207–1215.
O'CONNOR, C. J., DEAVER, B. S. JR. & SINN, E. (1979). *J. Chem. Phys.* **70**, 5161–5167.
ORTIZ, W. A., PADUAN-FILHO, A. & MISSELL, F. P. (1980). *Phys. Lett. A*, **77**, 183–184.
ORTIZ, W. A., PADUAN-FILHO, A. & MISSELL, F. P. (1981). *J. Mag. Magn. Mater.* **24**, 67–74.
PALACIO, F., PADUAN-FILHO, A. & CARLIN, R. L. (1980). *Phys. Rev. B*, **21**, 296–298.
SCHULTZ, A. J. (1987). *Trans. Am. Crystallogr. Assoc.* **23**, 61–69.
SCHULTZ, A. J., VAN DERVEER, D. G., PARKER, D. W. & BALDWIN, J. E. (1990). *Acta Cryst.* **C46**, 276–279.
SEARS, V. F. (1986). *Methods of Experimental Physics*, Vol. 23, *Neutron Scattering*, Part A, edited by K. SKÖLD & D. L. PRICE, pp. 521–550. Orlando: Academic Press.